Multivariable Control Problems

Coursework

Ashutosh Mukherjee

26.02.2023

Contents

Task 1: System Analysis

Question 1.1: Spectral decomposition

The transfer function of a state-space system $\mathbf{G(s)}$, can be expressed as equation (1.1),

$$\boldsymbol{G(s)} = \boldsymbol{C}\,(s\boldsymbol{I} - \boldsymbol{A})^{-1}\,\boldsymbol{B} + \boldsymbol{D}. \tag{1.1}$$

where $\boldsymbol{A}, \boldsymbol{B}, \boldsymbol{C}, \boldsymbol{D}$ are state-space matrices in minimum realization. Let $\boldsymbol{A}$ have no repeated eigenvalues. Then, from [5], $\boldsymbol{A}$ can be written as:

$$\boldsymbol{A} = \sum_{i=1}^{n} \lambda_i\, \boldsymbol{t}_i\, \boldsymbol{q}_i^H \tag{1.2}$$

According to the Shifting Theorem [2], the eigenvalues of $s\boldsymbol{I} - \boldsymbol{A}$ are $s - \lambda$ and the eigenvectors of $s\boldsymbol{I} - \boldsymbol{A}$ and $\boldsymbol{A}$ remain the same. Thus, we can write,

$$s\boldsymbol{I} - \boldsymbol{A} = \sum_{i=1}^{n} (s - \lambda_i)\, \boldsymbol{t}_i\, \boldsymbol{q}_i^H$$

Assuming all eigenvalues are non-zero, the eigenvalues of $\boldsymbol{A}^{-1}$ are $\{\frac{1}{\lambda_1}, \frac{1}{\lambda_2}...., \frac{1}{\lambda_n}\}$ and eigenvalues of $(s\boldsymbol{I} - \boldsymbol{A})^{-1}$ are $\{\frac{1}{s-\lambda_1}, \frac{1}{s-\lambda_2}...., \frac{1}{s-\lambda_n}\}$. Additionally, the same matrix diagonalizes $(s\boldsymbol{I} - \boldsymbol{A})^{-1}$ and $\boldsymbol{A}$ (Appendix A.2.1 in [5]). Thus, $(s\boldsymbol{I} - \boldsymbol{A})^{-1}$ and $\boldsymbol{A}$ will have the same eigenvectors. We can now write,

$$(s\boldsymbol{I} - \boldsymbol{A})^{-1} = \sum_{i=1}^{n} \frac{\boldsymbol{t}_i\, \boldsymbol{q}_i^H}{s - \lambda_i} \tag{1.3}$$

We know the input and output pole vectors as

$$\boldsymbol{y}_{pi} = \boldsymbol{C}\boldsymbol{t_i}$$
$$\boldsymbol{u}_{pi} = \boldsymbol{q}_i^H \boldsymbol{B}$$

Thus, equation (1.1) can be reformulated as,

$$\begin{aligned}
\boldsymbol{G(s)} &= \boldsymbol{C}\,(s\boldsymbol{I} - \boldsymbol{A})^{-1}\,\boldsymbol{B} + \boldsymbol{D} \\
&= \boldsymbol{C} \sum_{i=1}^{n} \frac{\boldsymbol{t}_i\, \boldsymbol{q}_i^H}{(s - \lambda_i)}\, \boldsymbol{B} + \boldsymbol{D} \\
&= \sum_{i=1}^{n} \frac{\boldsymbol{C}\, \boldsymbol{t}_i\, \boldsymbol{q}_i^H\, \boldsymbol{B}}{s - \lambda_i} + \boldsymbol{D} \\
&= \sum_{i=1}^{n} \frac{\boldsymbol{y}_{pi}\, \boldsymbol{u}_{pi}^H}{s - \lambda_i} + \boldsymbol{D}
\end{aligned}$$

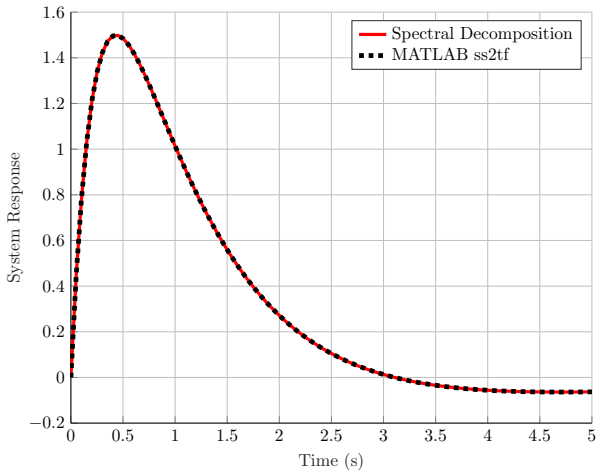

Figure 1.1: SISO Plant Response to a decaying input, $u = 2e^{-t}$.

Hence, proven.

Testing for a random plant $\boldsymbol{A}$ with 3 states:

$$\boldsymbol{A} = \begin{bmatrix} 2 & 1 & -0.5 \\ 1 & -1 & 0 \\ -0.5 & 0 & -4 \end{bmatrix}$$

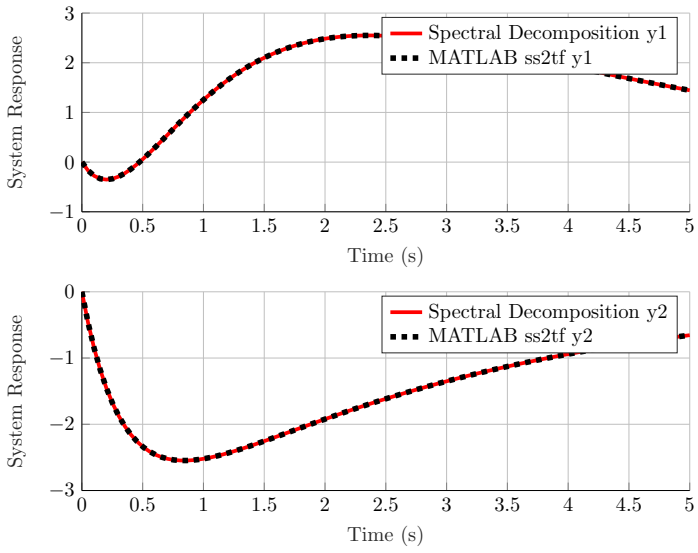

Figure 1.2: MIMO Plant Response to a decaying input, $u = [2e^{-t}\ 0]^T$.

in the case of SISO;

$$\boldsymbol{B} = \begin{bmatrix} 1 \\ 0 \\ 2 \end{bmatrix}, \boldsymbol{C} = \begin{bmatrix} 1 & -1 & 2 \end{bmatrix}, \boldsymbol{D} = \boldsymbol{0}$$

and MIMO (TITO);

$$\boldsymbol{B} = \begin{bmatrix} -1 & 0 \\ 4 & -2 \\ 0 & 1 \end{bmatrix}, \boldsymbol{C} = \begin{bmatrix} 2 & 0 & 0 \\ 1 & -1 & 2 \end{bmatrix}, \boldsymbol{D} = \begin{bmatrix} 0 & 0 \\ 0 & 0 \end{bmatrix}$$

As both figures 1.1 and 1.2 show, the spectral decomposition and the standard *ss2tf()* function in matlab leads to the same plants with the same responses to inputs.

Question 1.2: Repeated Eigenvalues

The *Jordan Decomposition Theorem* states that for any real or complex square matrix **A**, there exists an invertible **P** such that:

$$\boldsymbol{A} = \boldsymbol{P}\,\boldsymbol{J}\,\boldsymbol{P}^{-1} \tag{1.4}$$

where,

$$\boldsymbol{J} = \begin{bmatrix} \boldsymbol{J}_{k_1}(\lambda_1) & \dots & \dots & 0 \\ \vdots & \boldsymbol{J}_{k_2}(\lambda_2) & \dots & 0 \\ \vdots & \vdots & \ddots & \vdots \\ 0 & 0 & \dots & \boldsymbol{J}_{k_m}(\lambda_m) \end{bmatrix}, \boldsymbol{J}_{k_i}(\lambda_i) = \begin{bmatrix} \lambda_1 & 1 & 0 & \dots & 0 \\ \vdots & \lambda_2 & 1 & \dots & \vdots \\ \vdots & \vdots & \vdots & \ddots & \vdots \\ 0 & 0 & 0 & \dots & \lambda_i \end{bmatrix}$$

and, k_i: Multiplicity of i^{th} eigenvalue and **A** has m unique eigenvalues and $\boldsymbol{v_i}$: i^{th} generalized eigenvector of **A**. We know,

$$\boldsymbol{P} = \begin{bmatrix} \boldsymbol{v}_1 & \boldsymbol{v}_2 & \dots & \boldsymbol{v}_2 \end{bmatrix} = \begin{bmatrix} \boldsymbol{V}_1 & \boldsymbol{V}_2 & \dots & \boldsymbol{V}_m \end{bmatrix}$$

where $\dim(\boldsymbol{V}_i) = n\text{x}k_i$, and $\boldsymbol{V_i} = \begin{bmatrix} \boldsymbol{v}_{i_1} & \boldsymbol{v}_{i_2} & \dots & \boldsymbol{v}_{i_{k_m}} \end{bmatrix}$ where $\{\boldsymbol{v}_{i_1}, \boldsymbol{v}_{i_1} ... \boldsymbol{v}_{i_m}\}$ form the eigenspace of **A** and $\boldsymbol{v}_{i_1}$ is the ordinary eigenvector and the rest are generalized eigenvectors which are dependent on $\boldsymbol{v}_{i_1}$. Let **A** be limited to symmetric matrices. For symmetric matrices, we know that eigenvectors are always mutually orthogonal, even if eigenvalues are repeated. Thus **P** is orthogonal and equation 1.4 can be written as,

$$\boldsymbol{A} = \begin{bmatrix} \boldsymbol{V_1} & \boldsymbol{V_2} & \dots & \boldsymbol{V_m} \end{bmatrix} \begin{bmatrix} \boldsymbol{J}_{k_1}(\lambda_1) & \dots & \dots & 0 \\ \vdots & \boldsymbol{J}_{k_2}(\lambda_2) & \dots & 0 \\ \vdots & \vdots & \ddots & \vdots \\ 0 & 0 & \dots & \boldsymbol{J}_{k_m}(\lambda_m) \end{bmatrix} \begin{bmatrix} \boldsymbol{V_1}^H \\ \boldsymbol{V_2}^H \\ \vdots \\ \boldsymbol{V_m}^H \end{bmatrix}$$

$$\implies \boldsymbol{A} = \begin{bmatrix} \boldsymbol{V_1} & \boldsymbol{V_2} & \dots & \boldsymbol{V_m} \end{bmatrix} \begin{bmatrix} \boldsymbol{J}_{k_1}(\lambda_1)\,\boldsymbol{V_1^H} \\ \boldsymbol{J}_{k_2}(\lambda_2)\,\boldsymbol{V_2^H} \\ \vdots \\ \boldsymbol{J}_{k_m}(\lambda_m)\,\boldsymbol{V_m^H} \end{bmatrix}$$

$$= \sum_{i=1}^{m} \boldsymbol{V_i}\,\boldsymbol{J_{k_i}}(\lambda_i)\,\boldsymbol{V_i^H}$$

$$= \sum_{i=1}^{m} \begin{bmatrix} \boldsymbol{v}_{i_1} & \boldsymbol{v}_{i_2} & \dots & \boldsymbol{v}_{i_{ki}} \end{bmatrix} \begin{bmatrix} \lambda_i\,\boldsymbol{v}_{i_1}^H + \boldsymbol{v}_{i_2}^H \\ \lambda_i\,\boldsymbol{v}_{i_2}^H + \boldsymbol{v}_{i_3}^H \\ \vdots \\ \lambda_i\,\boldsymbol{v}_{i_{k_i-1}}^H + \boldsymbol{v}_{i_{k_i}}^H \\ \lambda_i\,\boldsymbol{v}_{i_{k_i}}^H \end{bmatrix}$$

$$= \sum_{i=1}^{m} \boldsymbol{v}_{i_1}\,\lambda_i\,\boldsymbol{v}_{i_1}^H + \boldsymbol{v}_{i_1}\,\boldsymbol{v}_{i_2}^H + \boldsymbol{v}_{i_2}\,\lambda_i\,\boldsymbol{v}_{i_2}^H + \boldsymbol{v}_{i_2}\,\boldsymbol{v}_{i_3}^H + \cdots + \lambda_i\,\boldsymbol{v}_{i_{k_i}}\,\boldsymbol{v}_{i_{k_i}}^H$$

$$= \sum_{i=1}^{m} \left[\left(\sum_{j=1}^{k_i-1} \boldsymbol{v}_{i_j}\,\lambda_i\,\boldsymbol{v}_{i_j}^H + \boldsymbol{v}_{i_j}\,\boldsymbol{v}_{i_{(j+1)}}^H \right) + \boldsymbol{v}_{i_{k_i}}\,\lambda_i\,\boldsymbol{v}_{i_{k_i}}^H \right]$$

Analogous to equation (1.3), we can write,

$$s\boldsymbol{I} - \boldsymbol{A} = \sum_{i=1}^{m} \left[\left(\sum_{j=1}^{k_i-1} \frac{\boldsymbol{v}_{i_j}\,\boldsymbol{v}_{i_j}^H}{s-\lambda_i} + \boldsymbol{v}_{i_j}\,\boldsymbol{v}_{i_{(j+1)}}^H \right) + \frac{\boldsymbol{v}_{i_{k_i}}\,\boldsymbol{v}_{i_{k_i}}^H}{s-\lambda_i} \right]$$

For a symmetric matrix, the left and right eigenvectors are the same. Thus, we can reformulate equation (1.1) as,

$$\boldsymbol{G}(\boldsymbol{s}) = \sum_{i=1}^{m} \left[\left(\sum_{j=1}^{k_i-1} \frac{\boldsymbol{C}\boldsymbol{t}_{i_j}\,\boldsymbol{q}_{i_j}^H\boldsymbol{B}}{s-\lambda_i} + \boldsymbol{C}\boldsymbol{t}_{i_j}\,\boldsymbol{t}_{i_{(j+1)}}^H\boldsymbol{B} \right) + \frac{\boldsymbol{C}\boldsymbol{t}_{i_{k_i}}\,\boldsymbol{q}_{i_{k_i}}^H\boldsymbol{B}}{s-\lambda_i} \right] + \boldsymbol{D}$$

$$= \sum_{i=1}^{m} \left[\left(\sum_{j=1}^{k_i-1} \frac{\boldsymbol{y}_{p_{i_j}}\,\boldsymbol{u}_{p_{i_j}}^H}{s-\lambda_i} + \boldsymbol{y}_{p_{i_j}}\,\boldsymbol{u}_{p_{i_{(j+1)}}}^H \right) + \frac{\boldsymbol{y}_{p_{i_{k_i}}}\,\boldsymbol{u}_{p_{i_{k_i}}}^H}{s-\lambda_i} \right] + \boldsymbol{D}$$

Question 1.3: System perturbation

The closed-loop transfer functions can be formulated as:

$$\begin{bmatrix} \boldsymbol{e}_1 \\ \boldsymbol{e}_2 \end{bmatrix} = \begin{bmatrix} \boldsymbol{H}_1 & \boldsymbol{H}_2 \\ \boldsymbol{H}_3 & \boldsymbol{H}_4 \end{bmatrix} \begin{bmatrix} \boldsymbol{w}_1 \\ \boldsymbol{w}_2 \end{bmatrix}$$

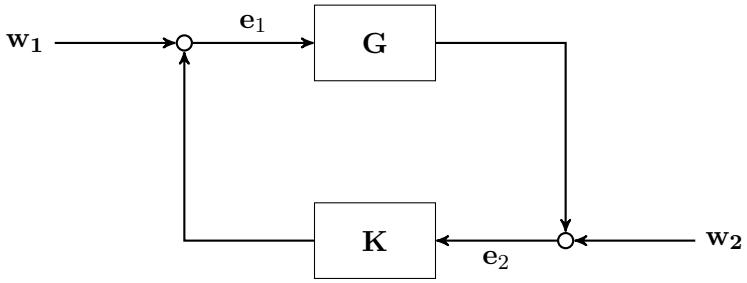

Figure 1.3: Feedback Control Loop.

For the feedback system,

$$\begin{aligned}\boldsymbol{e}_1 &= \boldsymbol{w}_1 + \boldsymbol{K}\boldsymbol{e}_2 \\ &= \boldsymbol{w}_1 + \boldsymbol{K}\left(\boldsymbol{w}_2 + \boldsymbol{G}\boldsymbol{e}_1\right) \\ &= \left(\boldsymbol{I} - \boldsymbol{K}\boldsymbol{G}\right)^{-1}\boldsymbol{w}_1 + \boldsymbol{K}\left(\boldsymbol{I} - \boldsymbol{G}\boldsymbol{K}\right)^{-1}\boldsymbol{w}_2 \Leftrightarrow \boldsymbol{H}_1 = \left(\boldsymbol{I} - \boldsymbol{K}\boldsymbol{G}\right)^{-1}, \boldsymbol{H}_2 = \boldsymbol{K}\left(\boldsymbol{I} - \boldsymbol{G}\boldsymbol{K}\right)^{-1}\end{aligned}$$

where

$$\boldsymbol{G} = \begin{bmatrix} 7 & 8 \\ 6 & 7 \end{bmatrix}\begin{bmatrix} \frac{1}{s+1} & 0 \\ 0 & \frac{2}{s+2} \end{bmatrix}\begin{bmatrix} 7 & 8 \\ 6 & 7 \end{bmatrix}^{-1}$$

Similarly, we can derive $\boldsymbol{H}_3$ and $\boldsymbol{H}_4$ and our closed loop system becomes

$$\begin{bmatrix} \boldsymbol{e}_1 \\ \boldsymbol{e}_2 \end{bmatrix} = \begin{bmatrix} \left(\boldsymbol{I} - \boldsymbol{K}\boldsymbol{G}\right)^{-1} & \boldsymbol{K}\left(\boldsymbol{I} - \boldsymbol{G}\boldsymbol{K}\right)^{-1} \\ \boldsymbol{G}\left(\boldsymbol{I} - \boldsymbol{K}\boldsymbol{G}\right)^{-1} & \left(\boldsymbol{I} - \boldsymbol{G}\boldsymbol{K}\right)^{-1} \end{bmatrix}\begin{bmatrix} \boldsymbol{w}_1 \\ \boldsymbol{w}_2 \end{bmatrix}$$

For $\boldsymbol{K} = -\boldsymbol{I}$, $\boldsymbol{K}\boldsymbol{G}$ and $\boldsymbol{G}\boldsymbol{K}$ have no RHP Pole-Zero cancellations, thus it is enough to

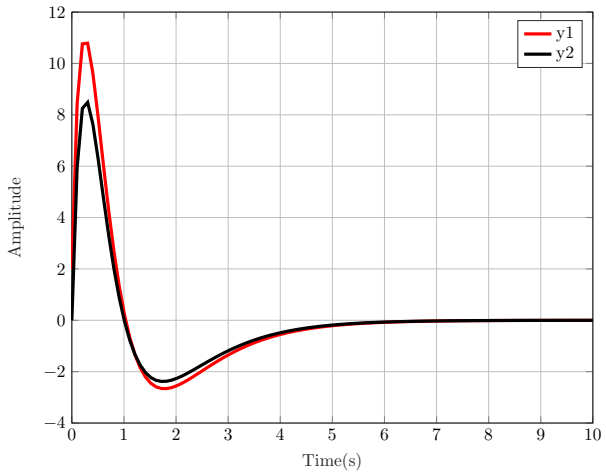

Figure 1.4: Output response of $\boldsymbol{H}_1$ to $\boldsymbol{u} = \begin{bmatrix} 2e^{-t} & 0 \end{bmatrix}^T$.

check the stability of one of the closed-loop transfer functions to determine the internal stability of the closed-loop system [6].

As seen in Figure 1.4, $\boldsymbol{H}_1$ is stable, thus our closed-loop system will be internally stable as well.

Modelling Dynamic Uncertainty

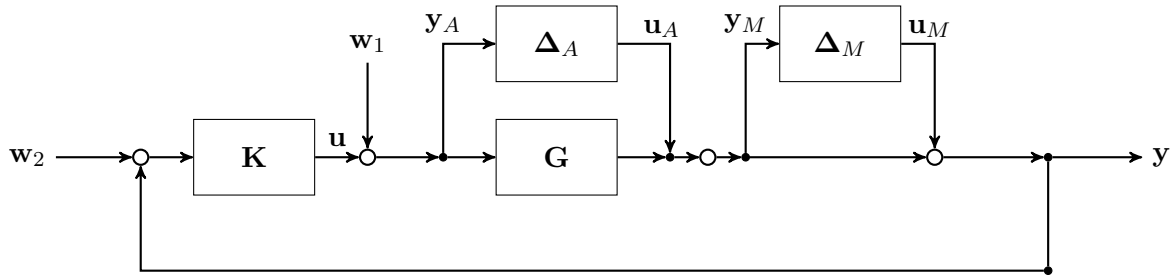

Figure 1.5: Uncertain System with Additive and Output Multiplicative Uncertainty.

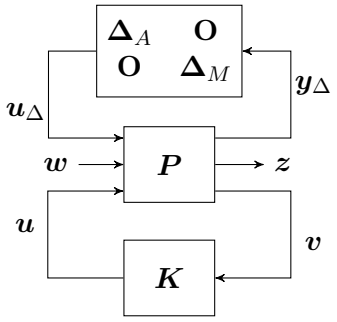

Figure 1.6: Generalized Uncertain Closed Loop Configuration with Dynamic Uncertainty.

The block diagram in Figure 1.5 can be rearranged in as the $\mathbf{M\Delta}$ structure with the perturbation matrix being set as

$$\boldsymbol{\Delta} = \begin{bmatrix} \boldsymbol{\Delta}_A & \mathbf{O} \\ \mathbf{O} & \boldsymbol{\Delta}_M \end{bmatrix}$$

Thus, $\boldsymbol{\Delta}$ is a structured perturbation with a block diagonal structure. The uncertainty and the controller can be taken out of the system, as shown in Figure 1.6. The generalized plant $\mathbf{P}$ can then be derived by the procedure as described in Chapter-8 of [5]. Assuming,

$$\boldsymbol{z} = \boldsymbol{y}$$
$$\boldsymbol{w} = \begin{bmatrix} \boldsymbol{w}_1 \\ \boldsymbol{w}_2 \end{bmatrix}$$

Our generalized plant will be,

$$\boldsymbol{P} = \begin{bmatrix} \boldsymbol{O} & \boldsymbol{O} & \boldsymbol{I} & \boldsymbol{O} & \boldsymbol{I} \\ \boldsymbol{I} & \boldsymbol{O} & \boldsymbol{G} & \boldsymbol{O} & \boldsymbol{G} \\ \boldsymbol{I} & \boldsymbol{I} & \boldsymbol{G} & \boldsymbol{O} & \boldsymbol{G} \\ \boldsymbol{I} & \boldsymbol{I} & \boldsymbol{G} & \boldsymbol{I} & \boldsymbol{G} \end{bmatrix}$$

The nominal closed-loop system can be obtained by closing the lower loop using a lower LFT,

$$\boldsymbol{N} = \mathcal{F}_l(\boldsymbol{P}, \boldsymbol{K})$$

Since, $\boldsymbol{M}$ maps $\boldsymbol{u}_\Delta$ to $\boldsymbol{y}_\Delta$, thus

$$\boldsymbol{M} = \boldsymbol{N}_{11} = \begin{bmatrix} \boldsymbol{KS} & \boldsymbol{KS} \\ \boldsymbol{I} + \boldsymbol{T} & \boldsymbol{T} \end{bmatrix}$$

where, $\boldsymbol{S} = (\boldsymbol{I} - \boldsymbol{GK})^{-1}$ and $\boldsymbol{T} = \boldsymbol{GK}\,(\boldsymbol{I} - \boldsymbol{GK})^{-1}$

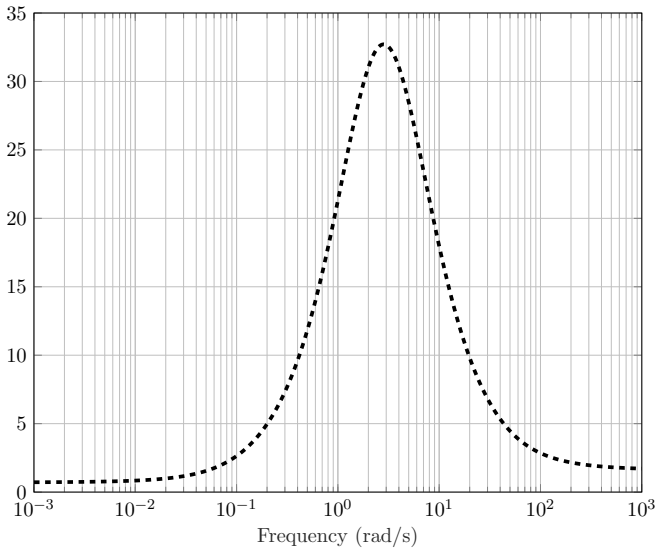

Figure 1.7: Singular Value Plot for the upper singular values of $\mathbf{M}$.

As seen in Figure 1.7, the $\mathcal{H}_\infty$ norm of $\mathbf{M}$ lies just below 33, which can be considered the worst-case perturbation ($\gamma = 33$) for the given structured dynamic uncertainty. The frequency at which this worst-case occurs is 2.8313 rad/s ($\omega^* = 2.8313$).

Modelling Perturbation Matrix

Let

$$\boldsymbol{\Delta}_A = \delta_A \boldsymbol{I}$$
$$\boldsymbol{\Delta}_M = \delta_M \boldsymbol{I}$$

where $\delta_A, \delta_M \in \mathbb{C}$. If both δ_A and δ_A are considered to be *all-pass* elements, such that,

$$\delta_A = \gamma \left(\frac{s-2}{s+2} \right), \delta_M = 0.01 \left(\frac{s-2}{s+2} \right)$$

$$\bar{\sigma} \left(\boldsymbol{\Delta}(j\omega^*) \right) = \gamma$$
$$\|\boldsymbol{\Delta}\|_\infty = \gamma, \boldsymbol{\Delta} \in \mathcal{RH}_\infty$$

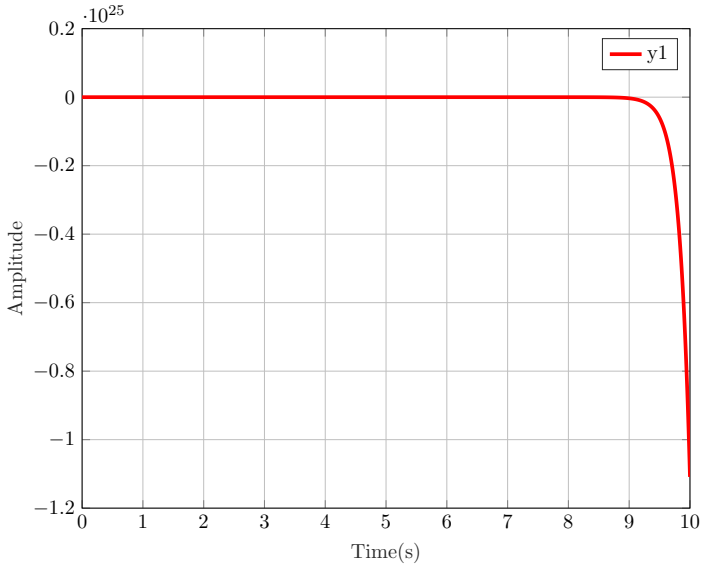

Figure 1.8: Reponse of the first output of the interconnection between $\mathbf{N}$ and $\boldsymbol{\Delta}$ to step input.

The interconnection between the closed-loop and $\boldsymbol{\Delta}$ is given by

$$\boldsymbol{F} = \mathcal{F}_u(\boldsymbol{N}, \boldsymbol{\Delta})$$

which is unstable, as seen in Figure 1.8.

Task 2: MIMO-systems

Question 2.1: Proof of equivalence

Average power of any random process $x(t)$,

$$P_X = E\left\{ \lim_{T\to\infty} \frac{1}{2T} \int_{-T}^{T} x(t)^2 \, dt \right\}$$

For a stochastic stationary process,

$$\begin{aligned} P_X &= \lim_{T\to\infty} \frac{1}{2T} \int_{-T}^{T} E\Big\{ x(t)^2 \Big\} dt \\ &= R_X(\tau = 0) \end{aligned}$$

where, $R(.)$ is the *Auto-Correlation functon*, and $\mathbf{R}_X = E\Big\{ \boldsymbol{X}(t+\tau)\boldsymbol{X}(t)^H \Big\}$, if $\boldsymbol{X}(t)$ is a random vector.

Average power of $\boldsymbol{z}(t)$:

$$P_z = E\left\{ \lim_{T\to\infty} \frac{1}{2T} \int_{-T}^{T} \boldsymbol{z}(t)^T \, \boldsymbol{z}(t) dt \right\} \tag{2.1}$$

which can be written as,

$$\begin{aligned} P_z &= \lim_{T\to\infty} \frac{1}{2T} \int_{-T}^{T} E\Big\{ \|\boldsymbol{z}(t)\|^2 \Big\} dt \\ &= \mathrm{Tr}\, \boldsymbol{R}_z(\tau = 0) \\ &= \mathrm{Tr}\, E\Big\{ \boldsymbol{z}(t)\boldsymbol{z}(t)^H \Big\} \end{aligned}$$

Hence, the first statement is proved.

The *spectral power density* represents the intensity of the signal, and is obtained when a Forward Fourier Transform is carried out on the Auto-correlation Function i.e. Spectral Power Density is the Auto-Correlation Function in the frequency domain. Thus,

$$\begin{aligned} \boldsymbol{R}_X &= \frac{1}{2\pi} \int_{-\infty}^{\infty} \boldsymbol{S}_X(j\omega) \, e^{j\omega\tau} \, d\omega \\ P_X &= \mathrm{Tr}\, \boldsymbol{R}_X(\tau = 0) \\ &= \frac{1}{2\pi} \int_{-\infty}^{\infty} \mathrm{Tr}(\boldsymbol{S}_X(j\omega)) \, d\omega \end{aligned}$$

For a stable LTI system, if $\boldsymbol{z} = \boldsymbol{F}\boldsymbol{w}$, then

$$\boldsymbol{S}_z = \boldsymbol{F}\boldsymbol{S}_w\boldsymbol{F}^H$$

and

$$P_z = \frac{1}{2\pi}\int_{-\infty}^{\infty} \mathrm{Tr}[\boldsymbol{F}(j\omega)\boldsymbol{S}_w(j\omega)\boldsymbol{F}(j\omega)^H]\, d\omega \tag{2.2}$$

Now, let $\boldsymbol{w}(t)$ be white noise of unit intensity, thus $\boldsymbol{S}_w(j\omega) = \boldsymbol{I}$ and $\boldsymbol{R}_w(\tau) = \boldsymbol{I}\delta(t-\tau) = E\Big\{\boldsymbol{w}(t)\boldsymbol{w}(t)^T\Big\}$, thus equation (2.2) can be written as,

$$\begin{aligned} P_z &= \frac{1}{2\pi}\int_{-\infty}^{\infty} \mathrm{Tr}[\boldsymbol{F}(j\omega)\boldsymbol{F}(j\omega)^H]\, d\omega \\ &= ||\boldsymbol{F}(s)||_2^2 \\ &= ||\mathcal{F}_l(\boldsymbol{P},\boldsymbol{K})||^2 \end{aligned}$$

Question 2.2: System zero and down squaring

The system has 2 inputs and 1 output, so a transfer function matrix with 1 row and 2 columns is expected for the plant. We convert the state space realization to the transfer function form using equation (1.1):

$$\boldsymbol{G}(s) = \begin{bmatrix} \frac{s-1}{s-2} & \frac{s+1}{s+2} \end{bmatrix}$$

Transmission Zeros

We can use the *McFarlane and Karcanias* approach as described in Chapter 4 of [5]. To that end, we need to first calculate the characteristic polynomial, the least common divisor of the denominators of all minors of all orders. Since for the plant, only minors of order 1 are possible,

$$\begin{aligned} &M_1 = \frac{s-1}{s-2}\,,\; M_2 = \frac{s+1}{s+2} \\ &\Phi(s) = (s-2)(s+2) \end{aligned}$$

The zero polynomial then can be obtained by writing the minors of order 1 in such a way that the characteristic polynomial is the denominator and calculating the greatest common divisor of the numerators. Thus,

$$M_1 = \frac{(s-1)(s+2)}{\Phi(s)}\,,\; M_2 = \frac{(s+1)(s-2)}{\Phi(s)}$$

Since there exists no common factor between the numerators of M_1 and M_2, we conclude that there is no transmission zero in the system. Additionally, to confirm our result, we

can check the *Rosenbrock matrix*, which is a polynomial matrix given by,

$$\boldsymbol{P}(s) = \begin{bmatrix} s\boldsymbol{I} - \boldsymbol{A} & -\boldsymbol{B} \\ \boldsymbol{C} & \boldsymbol{D} \end{bmatrix} = \begin{bmatrix} s-2 & 0 & -1 & 0 \\ 0 & s+2 & 0 & -1 \\ 1 & -1 & 1 & 1 \end{bmatrix}$$

The normal rank of **P** is 3. The existence of a transmission zero would make **P** rank-deficient at the zero locations. In order to induce rank deficiency, either 2 columns of **P** need to be dependent, or 1 row needs to be dependent. It can be seen that all rows are independent irrespective of s, while $s = 1$ and $s = -1$ lead to only 1 dependent column. Thus, **P** is always full rank, and there is no transmission zero in the system.

Pre-compensator Design

The pre-compensated plant will be given by,

$$\boldsymbol{G}_S = \boldsymbol{G}\boldsymbol{k}$$

where **k** is the pre-compensator gain matrix. Let

$$\begin{aligned} \boldsymbol{k} &= \begin{bmatrix} k1 \\ k2 \end{bmatrix} \\ G_S(s) &= k_1 \left(\frac{s-1}{s-2} \right) + k_2 \left(\frac{s+1}{s+2} \right) \\ z(s) &= k_1(s-1)(s+2) + k_2(s+1)(s-2) \\ \Phi(s) &= (s-2)(s+2) \end{aligned}$$

where $z(s)$ and $\Phi(s)$ are the zero and characteristic polynomials respectively. k_1 and k_2 can be set in such a way that pole-zero cancellations are induced but in the open LHP. To that end, let

$$\begin{aligned} k_1 = \alpha,\ k_2 = \beta \left(\frac{s+2}{s-2} \right) \\ G_S(s) = \frac{(\alpha+\beta)\, s + (\beta - \alpha)}{s-2} \end{aligned}$$

For $\beta > \alpha > 0$, the system zero is in the open LHP. Additionally, the above design ensures there is no RHP Pole-Zero cancellations.

Question 2.3: Euclids algorithm

The given transfer function can be factorised as follows:

$$G(s) = \frac{s-1}{(s+2)(s-2)(s+1)} \tag{2.3}$$

The procedure using Euclid's algorithm is followed, as given in Chapter 5 of [3]. Let

$$s = \frac{1-\lambda}{\lambda}$$

Then, G(s) can be transformed in λ as,

$$\tilde{G}(\lambda) = \frac{\lambda^2(1-2\,\lambda)}{(1-\lambda)(1-3\,\lambda)} = \frac{n(\lambda)}{m(\lambda)}$$

where $n(\lambda)$ and $m(\lambda)$ are coprime polynomials:

$$n(\lambda) = \lambda^2 - 2\,\lambda^3\,,\; m(\lambda) = 1 - 2\,\lambda - 3\,\lambda^2$$

Iteration 1

$$n = mq_1 + r_1$$
$$q_1 = \frac{2\lambda}{3} - \frac{7}{9}\,,\; r_1 = \frac{7}{9} - \frac{20\lambda}{9}$$

Iteration 2

$$m = r_1 q_2 + r_2$$
$$q_2 = \frac{27\lambda}{20} + \frac{549}{400}\,,\; r_2 = \frac{-27}{400}$$

Since r_2 is a non-zero constant, the algorithm is stopped. Now,

$$r_2 = -q_2 n + (1 + q_1 q_2)m$$
$$\left(\frac{-q_2}{r_2}\right) n + \left(\frac{1+q_1q_2}{r_2}\right) m = 1$$
$$u(\lambda) = \frac{-q_2}{r_2} = 20\lambda + \frac{61}{3}$$
$$v(\lambda) = \frac{1+q_1q_2}{r_2} = \frac{-40}{3}\lambda^2 + 2\lambda + 1$$

Retransforming back from λ to s, we get

$$N(s) = \frac{s-1}{(s+1)^3}$$
$$M(s) = \frac{(s+2)(s-2)}{(s+1)^2}$$
$$U(s) = \frac{61s+121}{3(s+1)}$$
$$V(s) = \frac{3s^2+12s-31}{3(s+1)^2}$$

$N(s)$ and $M(s)$ have no common RHP zeros, which is a necessary condition for coprime factorization. Additionally, $U(s)$ and $V(s)$ are semi-proper and stable, and it can be shown that for the obtained coprime transfer functions, the *Bezout's Identity* is satisfied.

Youla controller design

For $G(s)$, which is unstable and assumed to be in a negative feedback system, all internally stabilizing controllers are given by:

$$K(s) = (V - QN)^{-1}(U + QM)$$

where $Q(s) \in \mathcal{RH}_\infty$ and

$$V(s = \infty) - Q(s = \infty)N(s = \infty) \neq 0 \tag{2.4}$$

Let $Q(s) = \frac{1}{s+3}$ Now,

$$V(s = \infty) = \lim_{s\to\infty} \frac{31 - 12s - 3s^2}{3(s+1)^2} = -1$$
$$N(s = \infty) = \lim_{s\to\infty} \frac{s-1}{(s+1)^3} = 0$$

Thus, equation (2.4) never vanishes, irrespective of the value of $Q(s = \infty)$. We can

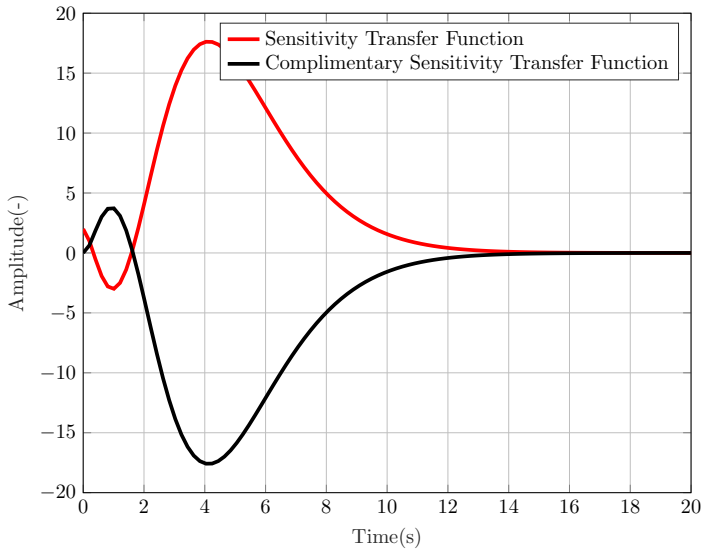

Figure 2.1: Response of closed-loop transfer functions a decaying input, $u = 2e^{-t}$.

represent the closed-loop transfer functions like $S(s)$ and $T(s)$ as affine functions of $Q(s)$. Assuming negative feedback,

$$S(s) = \frac{1}{1 + GK} = M(V - QN)$$
$$T(s) = \frac{GK}{1 + GK} = N(U + QM)$$

As seen in Figure 2.1, stable closed-loop transfer functions are obtained for the designed controller. Hence, it is possible to design a Youla controller to internally stabilise the system.

Task 3: Stability and LFT

Question 3.1: Stability and LFT

Parametric Uncertainty Modelling

The mass varies from -50% to 80% of the nominal mass value. We can model mass uncertainty as,

$$m_p = \frac{\bar{m} + b_m \Delta_m}{1 + d_m \Delta_m}, |\Delta_m| \leq 1$$
$$b_m = 0.385\bar{m}, d_m = -0.23$$

In a similar way, we can model spring stiffness and output gain, which vary with non-uniform bounds as the mass.

$$k_p = \frac{\bar{k} + b_k \Delta_k}{1 + d_k \Delta_m}, |\Delta_k| \leq 1$$
$$b_k = -0.28\bar{k}, d_k = -0.6$$
$$h_p = \frac{\bar{h} + b_h \Delta_h}{1 + d_h \Delta_h}, |\Delta_h| \leq 1$$
$$b_h = -0.28\bar{h}, d_h = -0.6$$

Since the damping varies with uniform bounds,

$$cp = \bar{c}\left(1 + r_c \Delta_c\right), |\Delta_c| \leq 1$$
$$r_c = \frac{c_{max} - c_{min}}{c_{max} + c_{min}}$$

Since these are parametric uncertainties, $\{\Delta_m, \Delta_c, \Delta_k, \Delta_h\} \in \mathbb{R}$. For any function $f(\delta)$ of the form,

$$f(\delta) = \frac{\alpha + \beta\delta}{1 + \gamma\delta}$$

we can use lower LFT to represent $f(\delta)$ [1] as,

$$f(\delta) = \mathcal{F}_l(\boldsymbol{M}, \delta), \boldsymbol{M} = \begin{bmatrix} \alpha & \beta - \alpha\gamma \\ 1 & -\gamma \end{bmatrix}$$
$$f^{-1}(\delta) = \mathcal{F}_l(\tilde{\boldsymbol{M}}, \delta), \tilde{\boldsymbol{M}} = \begin{bmatrix} \frac{1}{\alpha} & \frac{\gamma}{\alpha} - \frac{\beta}{\alpha^2} \\ 1 & \frac{-\beta}{\alpha} \end{bmatrix}$$

Thus, we can represent the parametric uncertainties in the form of lower LFTs with their respective Δs as,

$$m_p = \mathcal{F}_l\left(\begin{bmatrix} \frac{1}{\bar{m}} & \frac{d_m}{\bar{m}} - \frac{b_m}{\bar{m}^2} \\ 1 & \frac{-b_m}{\bar{m}} \end{bmatrix}, \Delta_m\right)$$

$$c_p = \mathcal{F}_l\left(\begin{bmatrix} \bar{c} & 1 \\ r_c\bar{c} & 0 \end{bmatrix}, \Delta_c\right)$$

$$k_p = \mathcal{F}_l\left(\begin{bmatrix} \bar{k} & b_k - \bar{k}d_k \\ 1 & -d_k \end{bmatrix}, \Delta_k\right)$$

$$h_p = \mathcal{F}_l\left(\begin{bmatrix} \bar{h} & b_h - \bar{h}d_h \\ 1 & -d_h \end{bmatrix}, \Delta_h\right)$$

Block Diagram

The system can be represented in block diagram form as done if Figure 3.1. Moreover, we can generalize the block diagram in form of a lower LFT and upper LFT as seen in Figure 3.2. In the generalized configuration, the following is considered,

$$\boldsymbol{\Delta} = \begin{bmatrix} \Delta_m & 0 & 0 & 0 \\ 0 & \Delta_c & 0 & 0 \\ 0 & 0 & \Delta_k & 0 \\ 0 & 0 & 0 & \Delta_m \end{bmatrix}, \boldsymbol{y}_\Delta = \begin{bmatrix} y_m \\ y_c \\ y_k \\ y_h \end{bmatrix}, \boldsymbol{u}_\Delta = \begin{bmatrix} u_m \\ u_c \\ u_k \\ u_h \end{bmatrix}$$

$$z = W_1 y, v = -y, \begin{bmatrix} \boldsymbol{y}_\Delta \\ \dot{\boldsymbol{x}} \\ z \\ v \end{bmatrix} = \boldsymbol{P} \begin{bmatrix} \boldsymbol{u}_\Delta \\ \boldsymbol{x} \\ d \\ u \end{bmatrix}$$

Analyzing the relations between different signals, the generalized plant $\mathbf{P}$ can be derived as,

$$\boldsymbol{P} = \begin{bmatrix} \frac{-b_m}{\bar{m}} & -1 & -(b_k - \bar{k}d_k) & 0 & -\bar{k} & -\bar{c} & 0 & 1 \\ 0 & 0 & 0 & 0 & 0 & r_c\bar{c} & 0 & 0 \\ 0 & 0 & -d_k & 0 & 1 & 0 & 0 & 0 \\ 0 & 0 & 0 & -d_h & 1 & 0 & 0 & 0 \\ 0 & 0 & 0 & 0 & 0 & 1 & 0 & 0 \\ \frac{d_m}{\bar{m}} - \frac{b_m}{\bar{m}^2} & \frac{-1}{\bar{m}} & \frac{-(b_k - \bar{k}d_k)}{\bar{m}} & 0 & \frac{-\bar{k}}{\bar{m}} & \frac{-\bar{c}}{\bar{m}} & 0 & \frac{1}{\bar{m}} \\ 0 & 0 & 0 & W_1(b_h - \bar{h}d_h) & W_1\bar{h} & 0 & W_1 & 0 \\ 0 & 0 & 0 & -(b_h - \bar{h}d_h) & -\bar{h} & 0 & -1 & 0 \end{bmatrix}$$

Note: *The above generalized plant matrix has been formed assuming W_2 is a part of the controller. If W_2 is considered a part of the plant, then it will populate the last column corresponding to row 1 and row 6 of the generalized plant matrix..*

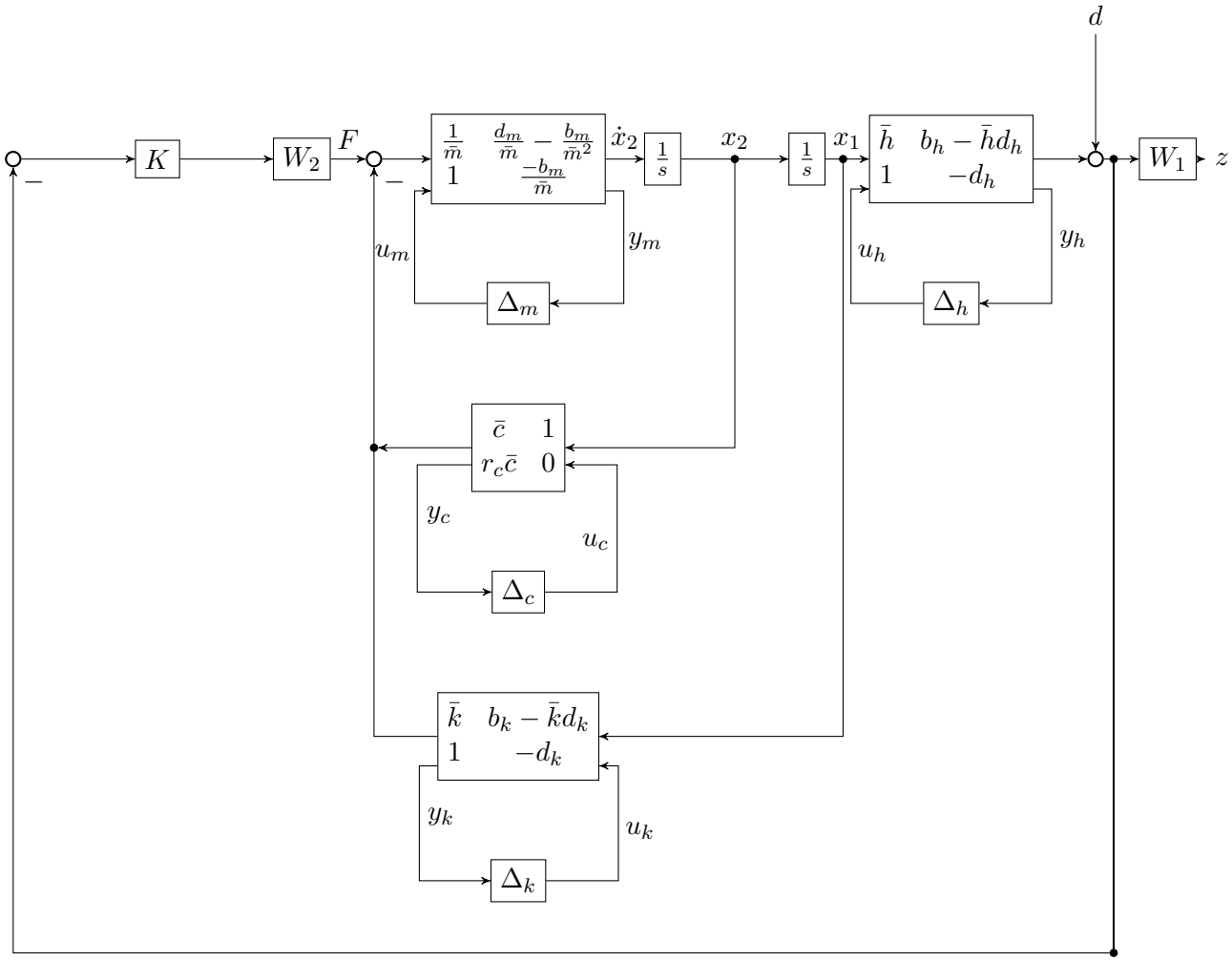

Figure 3.1: Block Diagram for the uncertain dynamic system.

The number of uncertainty channels in the system will be 4, corresponding to the 4 real parametric perturbations introduced. The above uncertain system is put into the *Robust Control Toolbox* in MATLAB, by inputting the following uncertain plant transfer function

$$G_p(s) = \frac{h_p}{m_p s^2 + c_p s + k_p}$$

The uncertain state space model in MATLAB obtained has 2 states, and 4 uncertainty output channels.

PI Controller Design

First the lag compensator is designed. τ is taken as 10, and k_0 is set such that the gain cross-over frequency is 1 rad/s. For such a condition, we obtain k_0 as 5.3547. A seperate

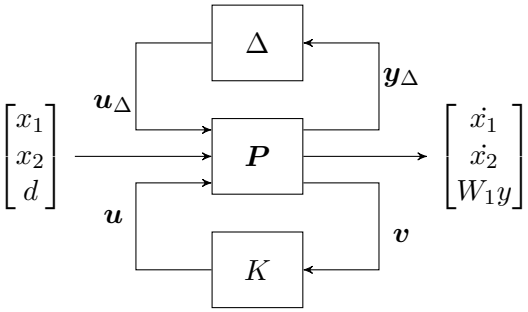

Figure 3.2: Generalized Uncertain Closed Loop Configuration with Parametric Uncertainty.

lead compensator is not designed for this controller, instead the output weight W_2 can be considered as a lead compensator with $T = 0.7$ and $\alpha = 0.1$. Thus, the lead-lag compensated PI controller is given by,

$$K(s) = 0.3k_0 \left(\frac{0.7s+1}{0.07s+1}\right)\left(\frac{10s+1}{10s}\right)$$

Robust Stability

We can obtain the unperturbed closed loop of the system with,

$$\boldsymbol{N} = \mathcal{F}_l(\boldsymbol{P}, K)$$

We also know that the $\mathbf{M}$ matrix which mapes $\boldsymbol{u}_\Delta$ to $\boldsymbol{y}_\Delta$ is,

$$\boldsymbol{M} = \boldsymbol{N}_{11}$$

In order to compute the robust stability using *Robust Control Toolbox*, the following uncertain transfer function mapping the disturbance signal to the exogenous output is used,

$$H(s) = \frac{W_1}{1 + \frac{W_1 h_p K}{m_p s^2 + c_p s + k_p}}$$

The command *lftdata(.)* is used to obtain the unperturbed closed loop system, and the $\mathbf{M}$ is obtained by taking the first 4 rows and columns of the closed loop system matrix.

Figure 3.3 shows us that the manually computed $\mathbf{M}$ has more conservatism than the one computed from *Robust Control Toolbox*. Additionally, since the perturbation matrix is structured in the form of a block diagonal matrix, it makes more sense to compute the *structured singular value* of $\mathbf{M}$, since the structured singular value consitutes the necessary and sufficient condition for RS when $\boldsymbol{\Delta}$ is structured. Figure 3.4 shows us that $\mu_\Delta(\mathbf{M})$ is roughly equal to 0.6, which implies RS.

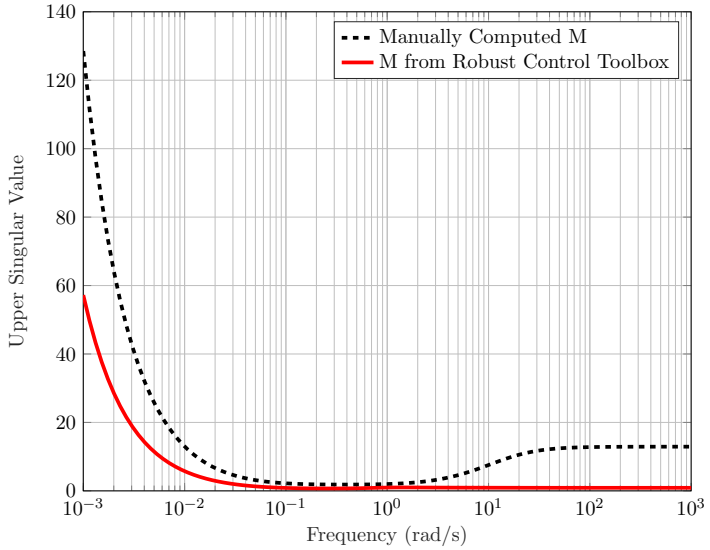

Figure 3.3: Comparison of the upper singular values of **M** computed manually with the one computed from *Robust Control Toolbox*.

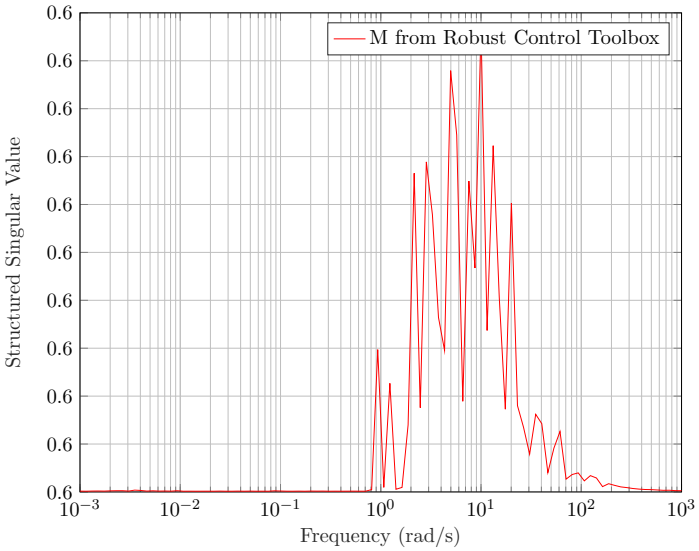

Figure 3.4: Structured singular values of **M** computed from *Robust Control Toolbox*.

Nominal Performance

Figure 3.5 shows us that $\bar{\sigma}(\mathbf{N}_{22}) > 1$, for higher frequencies which implies NP is not satisfied.

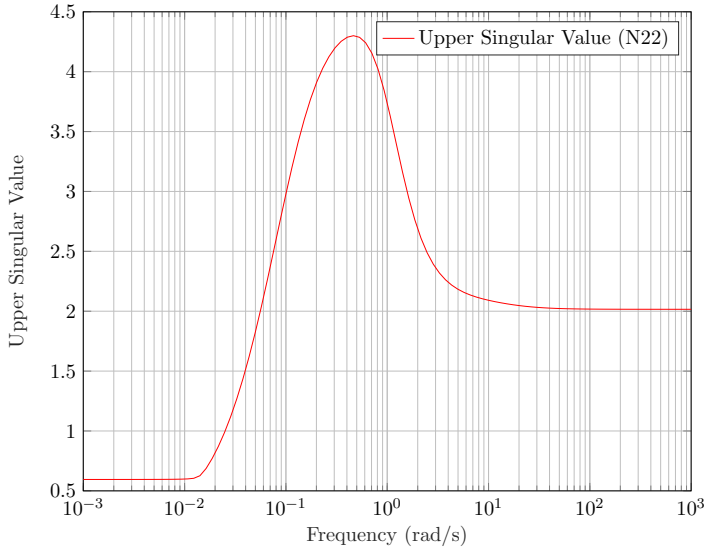

Figure 3.5: Upper singular values of $\mathbf{N}_{22}$.

Uncertain Time-Delay

Since the uncertain time-delay has uniform bounds, multiplicative uncertainty can be used to model the perturbation. Using first-order Pade´ approximation for the time delay, we have a standard form of multiplicative uncertainty weight to model Gain and Time-Delay Uncertainty, as proposed by Lundstörm [5],

$$w_M(s) = \frac{\left(1 + \frac{r_k}{2}\right)\tau_{max}s + r_k}{\frac{\tau_{max}}{2}s + 1}$$

Since there is only time-delay uncertainty, $r_k = 0$ and

$$w_\tau(s) = \frac{\tau_{max}s}{\frac{\tau_{max}}{2}s + 1}, \|\Delta_\tau(j\omega)\| \leq 1$$

$$G_p(s) = \left(\frac{h_p}{m_p s^2 + c_p s + k_p}\right) e^{-\tau_p s}$$

Figure 3.6 shows the generalised representation of the system with the additional time

delay uncertainty. The generalized plant is obtained as,

$$\boldsymbol{P} = \begin{bmatrix} \frac{-b_m}{\bar{m}} & -1 & -(b_k - \bar{k}d_k) & 0 & 1 & -\bar{k} & -\bar{c} & 0 & 1 \\ 0 & 0 & 0 & 0 & 0 & 0 & r_c\bar{c} & 0 & 0 \\ 0 & 0 & -d_k & 0 & 0 & 1 & 0 & 0 & 0 \\ 0 & 0 & 0 & -d_h & 0 & 1 & 0 & 0 & 0 \\ 0 & 0 & 0 & 0 & 0 & 1 & 0 & 0 & w_\tau \\ 0 & 0 & 0 & 0 & 0 & 0 & 1 & 0 & 0 \\ \frac{d_m}{\bar{m}} - \frac{b_m}{\bar{m}^2} & \frac{-1}{\bar{m}} & \frac{-(b_k - \bar{k}d_k)}{\bar{m}} & 0 & \frac{-1}{\bar{m}} & \frac{-\bar{k}}{\bar{m}} & \frac{-\bar{c}}{\bar{m}} & 0 & \frac{1}{\bar{m}} \\ 0 & 0 & 0 & W_1(b_h - \bar{h}d_h) & 0 & W_1\bar{h} & 0 & W_1 & 0 \\ 0 & 0 & 0 & -(b_h - \bar{h}d_h) & 0 & -\bar{h} & 0 & -1 & 0 \end{bmatrix}$$

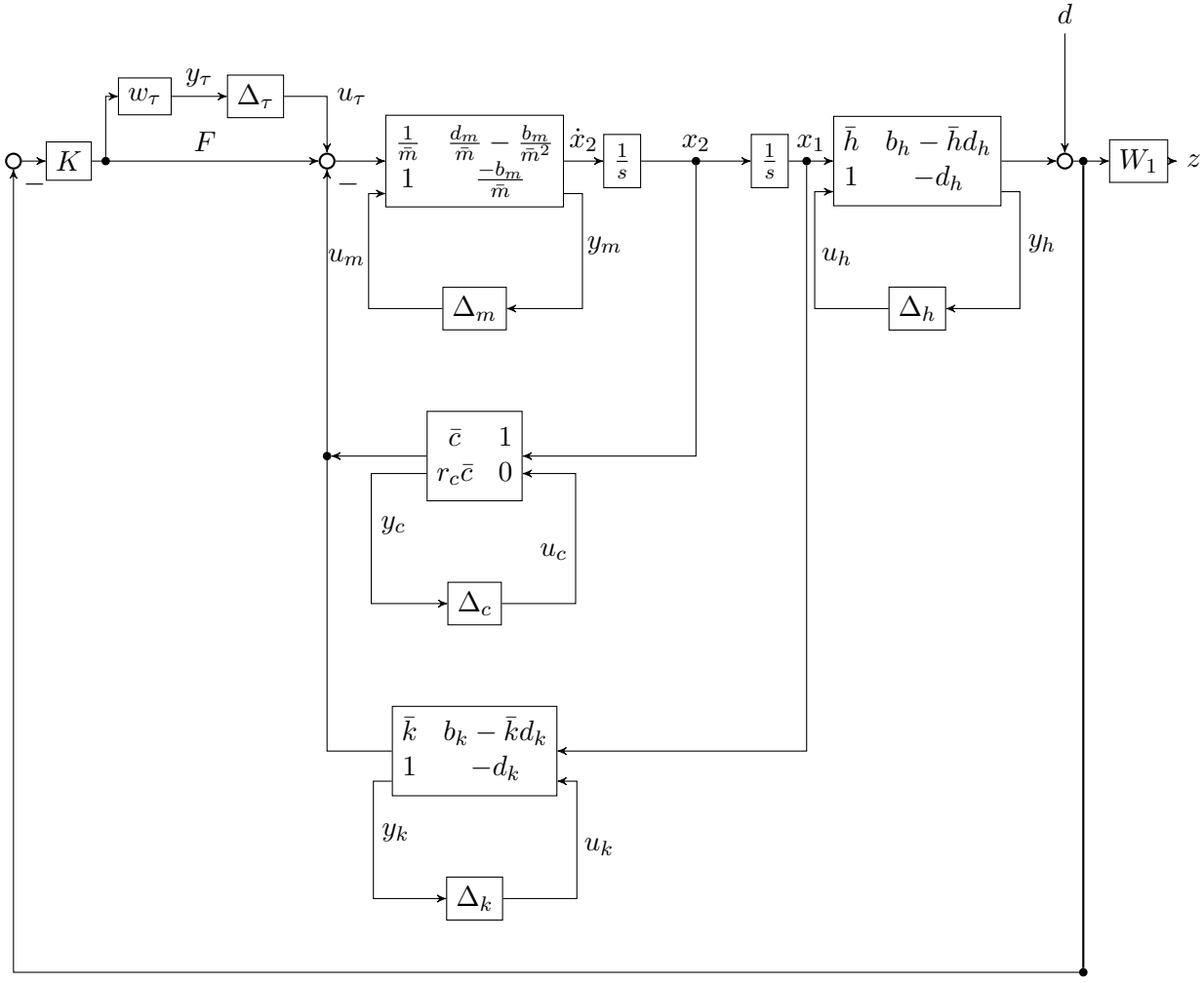

Figure 3.6: Block Diagram for the uncertain dynamic system with additional time-delay uncertainty.

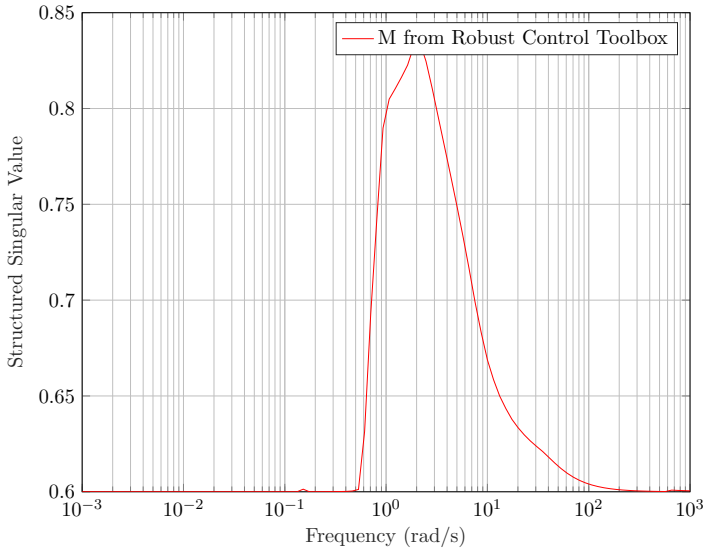

Figure 3.7: Structured singular values of $\mathbf{M}$ with added time delay uncertainty computed from *Robust Control Toolbox*.

It is found that the upper singular values of $\mathbf{M}$ and $\mathbf{N}_{22}$ stay roughly the same as compared to when there is no time delay. Hence, the time delay has no effect on the nominal performance. But as figure 3.7 shows, the robustness slightly decreases between the frequencies 0.61 rad/s and 100 rad/s.

Question 3.2: Linear fractional transformation

The transformation from $\mathbf{G}(s)$ to the state space is described by equation (1.1), which can be represented using a lower LFT [1] as,

$$\boldsymbol{G}(s) = \mathcal{F}_l\left(\begin{bmatrix}\boldsymbol{D} & \boldsymbol{C}\\ \boldsymbol{B} & \boldsymbol{A}\end{bmatrix}, \frac{1}{s}\boldsymbol{I}\right)$$

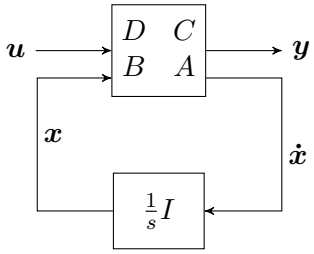

Figure 3.8: Lower LFT representing ss2tf

Considering the w-domain, we can write

$$\boldsymbol{G}(w) = \mathcal{F}_l\left(\begin{bmatrix}\hat{\boldsymbol{D}} & \hat{\boldsymbol{C}}\\ \hat{\boldsymbol{B}} & \hat{\boldsymbol{A}}\end{bmatrix}, \frac{1}{w}\boldsymbol{I}\right)$$

Using the concept of interconnection of LFTs (Appendix A.7.1 in [5]), we can further write equation (1.1) as,

$$\begin{aligned}\boldsymbol{G}(s) &= \mathcal{F}_l\left(\begin{bmatrix}\boldsymbol{D} & \boldsymbol{C}\\ \boldsymbol{B} & \boldsymbol{A}\end{bmatrix}, \frac{1}{s}\boldsymbol{I}\right)\\ &= \mathcal{F}_l\left(\begin{bmatrix}\boldsymbol{D} & \boldsymbol{C}\\ \boldsymbol{B} & \boldsymbol{A}\end{bmatrix}, \mathcal{F}_l\left(\boldsymbol{N}, \frac{1}{w}\boldsymbol{I}\right)\right)\\ &= \mathcal{F}_l\left(\begin{bmatrix}\hat{\boldsymbol{D}} & \hat{\boldsymbol{C}}\\ \hat{\boldsymbol{B}} & \hat{\boldsymbol{A}}\end{bmatrix}, \frac{1}{w}\boldsymbol{I}\right) = \hat{\boldsymbol{G}}(s)\end{aligned}$$

Now, using the transformation given between w and s, we can write,

$$\frac{1}{s} = \frac{cw - a}{b - dw}$$

and

$$\begin{aligned}\frac{1}{s}\boldsymbol{I} &= \left(\frac{cw-a}{b-dw}\right)\boldsymbol{I}\\ &= \frac{-c}{d}\boldsymbol{I} + \frac{(bc-ad)}{d(b-dw)}\boldsymbol{I}\\ &= \mathcal{F}_l\left(\boldsymbol{N}, \frac{1}{w}\boldsymbol{I}\right)\\ &= \boldsymbol{N}_{11} + \boldsymbol{N}_{12}\frac{1}{w}\left(\boldsymbol{I} - \frac{1}{w}\boldsymbol{N}_{22}\right)^{-1}\boldsymbol{N}_{21}\end{aligned}$$

Let $\mathbf{N}_{11} = -\frac{c}{d}\mathbf{I}$ and $\mathbf{N}_{22} = \frac{b}{d}\mathbf{I}$. Then,

$$\&bmN_{12}\frac{1}{w}\left(\boldsymbol{I} - \frac{1}{w}\frac{b}{d}\boldsymbol{I}\right)^{-1}\boldsymbol{N}_{21} = \frac{(bc-ad)}{d(b-dw)}\boldsymbol{I}$$

$$\implies \boldsymbol{N}_{12}\boldsymbol{N}_{21} = \left(\frac{ad-bc}{d^2}\right)\boldsymbol{I}$$

Let $\mathbf{N}_{12} = \left(a - \frac{bc}{d}\right)\mathbf{I}$ and $\mathbf{N}_{21} = \frac{1}{d}\mathbf{I}$ Then,

$$\frac{1}{s}\boldsymbol{I} = \mathcal{F}_l\left(\begin{bmatrix}-\frac{c}{d}\boldsymbol{I} & \left(a - \frac{bc}{d}\right)\boldsymbol{I}\\ \frac{1}{d}\boldsymbol{I} & \frac{b}{d}\boldsymbol{I}\end{bmatrix}, \frac{1}{w}\boldsymbol{I}\right)$$

Using formula A.156 from Appendix A.7.1 of [5], we can calculate,

$$\begin{aligned}
\hat{\boldsymbol{D}} &= \boldsymbol{D} - \boldsymbol{C}\left(\frac{c}{d}\right)\left(\boldsymbol{I} + \boldsymbol{A}\frac{c}{d}\right) \\
&= \boldsymbol{D} - c\boldsymbol{C}(d\boldsymbol{I} + c\boldsymbol{A})^{-1}\boldsymbol{B} \\
\hat{\boldsymbol{C}} &= \boldsymbol{C}\left(\boldsymbol{I} + \frac{c}{d}\boldsymbol{A}\right) - 1\left(a - \frac{bc}{d}\right)\boldsymbol{I} \\
&= (ad - bc)\boldsymbol{C}\left(c\boldsymbol{A} + d\boldsymbol{I}\right)^{-1} \\
\hat{\boldsymbol{B}} &= \frac{1}{d}\left(\boldsymbol{I} + \frac{c}{d}\boldsymbol{A}\right)^{-1} \\
&= \left(c\boldsymbol{A} + d\boldsymbol{I}\right)^{-1}\boldsymbol{B} \\
\hat{\boldsymbol{A}} &= \left(\frac{b}{d}\right)\boldsymbol{I} + \frac{1}{d}\boldsymbol{A}\left(\boldsymbol{I} + \frac{c}{d}\boldsymbol{A}\right)^{-1}\left(a - \frac{bc}{d}\right) \\
&= a\boldsymbol{A}(d\boldsymbol{I} + c\boldsymbol{A})^{-1} + b\left[\boldsymbol{I} - \frac{c}{d}\boldsymbol{A}(d\boldsymbol{I} + c\boldsymbol{A})^{-1}\right]
\end{aligned}$$

The inverse form (Pg. 301, [5]) can be used so that

$$\begin{aligned}
b\left[\boldsymbol{I} - \frac{c}{d}\boldsymbol{A}(d\boldsymbol{I} + c\boldsymbol{A})^{-1}\right] &= b(d\boldsymbol{I} + c\boldsymbol{A})^{-1} \\
\implies \hat{\boldsymbol{A}} &= (a\boldsymbol{A} + b\boldsymbol{I})\left(c\boldsymbol{A} + d\boldsymbol{I}\right)^{-1}
\end{aligned}$$

Controllability and Observability

$(\hat{\mathbf{A}}, \hat{\mathbf{B}})$ and $(\hat{\mathbf{A}}, \hat{\mathbf{C}})$ are controllable and observable iff,

$$\begin{aligned}
\hat{\boldsymbol{u}}_{pi} &= \hat{\boldsymbol{q}}_i^H\hat{\boldsymbol{B}} \neq 0, \forall i \in [1, n] \,\& \\
\hat{\boldsymbol{y}}_{pi} &= \hat{\boldsymbol{C}}\hat{\boldsymbol{t}}_i \neq 0, \forall i \in [1, n]
\end{aligned}$$

We know that the same eigenvectors diagonalize $\boldsymbol{A}$, $(c\boldsymbol{A} + d\boldsymbol{I})^{-1}$ and $a\boldsymbol{A} + b\boldsymbol{I}$. Then,

$$\begin{aligned}
\hat{\boldsymbol{A}} &= (a\boldsymbol{A} + b\boldsymbol{I})(c\boldsymbol{A} + d\boldsymbol{I})^{-1} = \left[\boldsymbol{Q}^{-1}(a\boldsymbol{A} + b\boldsymbol{I})\boldsymbol{Q}\right]\left[\boldsymbol{Q}^{-1}(c\boldsymbol{A} + d\boldsymbol{I})^{-1}\boldsymbol{Q}\right] \\
&= \boldsymbol{Q}^{-1}(a\boldsymbol{A} + b\boldsymbol{I})(c\boldsymbol{A} + d\boldsymbol{I})^{-1}\boldsymbol{Q}
\end{aligned}$$

Thus, $\hat{\boldsymbol{A}}$ and $\boldsymbol{A}$ have the same eigenvectors. Since $c\mathbf{A} + d\mathbf{I}$ is not singular,

$$\begin{aligned}
\hat{\boldsymbol{u}}_{pi} &= \boldsymbol{q}_i^H(c\boldsymbol{A} + d\boldsymbol{I})^{-1}\boldsymbol{B} \neq 0 \\
\implies \boldsymbol{q}_i^H &\neq 0 \,\&\, \boldsymbol{B} \neq 0, \forall i \in [1, n]
\end{aligned}$$

which is the necessary and sufficient condition for the controllability of $(\mathbf{A}, \mathbf{B})$. Thus, $(\hat{\mathbf{A}}, \hat{\mathbf{B}})$ is controllable iff $(\mathbf{A}, \mathbf{B})$ is controllable. The same can be shown for observability since $ad - bc \neq 0$,

$$\begin{aligned}
\hat{\boldsymbol{y}}_{pi} &= (ad - bc)\boldsymbol{C}\left(c\boldsymbol{A} + d\boldsymbol{I}\right)^{-1}\boldsymbol{t}_i \neq 0 \\
\implies \boldsymbol{t}_i &\neq 0 \,\&\, \boldsymbol{C} \neq 0, \forall i \in [1, n]
\end{aligned}$$

Thus, $(\hat{\mathbf{A}}, \hat{\mathbf{C}})$ is observable iff $(\mathbf{A}, \mathbf{C})$ is observable.

Task 4: Coprime Factorizations and Youla Parametrisation

Question 4.1: HIMAT example system analysis

The transfer function matrix reduced 4th-order system can be obtained from the reduced state-space matrices using Equation (1.1).

$$\boldsymbol{G}(s) = \begin{bmatrix} \frac{0.3384s^3-26.13s^2-0.3659s+0.01678}{s^4+3.068s^3-3.362s^2-0.5748s+0.7598} & \frac{-0.3349s^3+18.21s^2+0.3487s-0.05939}{s^4+3.068s^3-3.362s^2-0.5748s+0.7598} \\ \frac{0.4755s^3-25.3s^2-51.36s-1.387}{s^4+3.068s^3-3.362s^2-0.5748s+0.7598} & \frac{-0.3107s^3+17.81s^2+35.49s+1.027}{s^4+3.068s^3-3.362s^2-0.5748s+0.7598} \end{bmatrix}$$

All elements of $\mathbf{G}(s)$ have the same denominator polynomial, and the common denominator form can be written as,

$$\boldsymbol{G}(s) = \frac{1}{d(s)}\boldsymbol{N}(s)$$
$$d(s) = s^4 + 3.068s^3 - 3.362s^2 - 0.5748s + 0.7598$$
$$\boldsymbol{N} = \begin{bmatrix} 0.3384s^3 - 26.13s^2 - 0.3659s + 0.01678 & -0.3349s^3 + 18.21s^2 + 0.3487s - 0.05939 \\ 0.4755s^3 - 25.3s^2 - 51.36s - 1.387 & -0.3107s^3 + 17.81s^2 + 35.49s + 1.027 \end{bmatrix}$$

The smith form of the transfer function matrix is obtained using the *smithForm* inbuilt function in MATLAB.

$$\boldsymbol{S}(s) = \begin{bmatrix} \gamma_1^S(s) & 0 \\ 0 & \gamma_2^S(s) \end{bmatrix}$$
$$\gamma_1^S(s) = 1$$
$$\gamma_2^S(s) = (s + 0.0272)(s + 0.4742)(s - 0.5937)(s - 0.6951)(s + 3.383)(s - 58.2846)$$

The Smith-McMillan form can be obtained as,

$$\boldsymbol{M}(s) = \frac{1}{d(s)}\boldsymbol{S}(s)$$
$$\boldsymbol{M}(s) = \begin{bmatrix} \frac{\gamma_1(s)}{\beta_1(s)} & 0 \\ 0 & \frac{\gamma_2(s)}{\beta_2(s)} \end{bmatrix}$$
$$\gamma_1(s) = 1, \beta_1(s) = d(s)$$
$$\gamma_2(s) = (s + 0.0272)(s - 58.2846), \beta_2(s) = 1$$

The combined roots of $\gamma_1(s)$ and $\gamma_2(s)$ will give the transmission zeros of the system. Thus, it can be seen that $z = 58.2846$ is the added RHP zero in the reduced system.

It can be seen from Figure 4.1 that the condition number of the reduced-order model becomes higher than that of the full-order model, especially for $\omega \in [0.16, 1]$ rad/s. Additionally, the small value of the lower singular values in this frequency range (given that the condition number is high in this range) implies problems in control design [5].

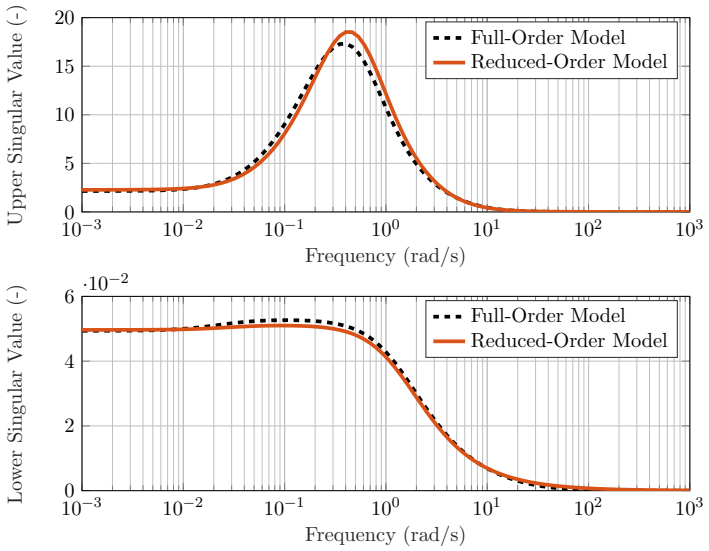

Figure 4.1: Singular Value plots of the full-order and reduced-order model.

Question 4.2: Coprime Factorization

The reduced system is given by,

$$\boldsymbol{G}(s) \stackrel{S}{=} \begin{bmatrix} \boldsymbol{A} & \boldsymbol{B} \\ \boldsymbol{C} & \boldsymbol{D} \end{bmatrix}$$

The pre-requisite for the Doubly Co-prime factorization of $\mathbf{G}(s)$ is that the system should have no hidden unstable modes [4]. To that end, the ranks of the controllability and observability matrices are computed in MATLAB using *Control System Toolbox* commands *crtb()* and *obsv()*. Both the matrices have a rank equal to the number of reduced states, thus there exist no unstable hidden modes. Let the doubly co-prime factorization of $\mathbf{G}(s)$ be given by,

$$\boldsymbol{G}(s) = \boldsymbol{N}\boldsymbol{M}^{-1} = \tilde{\boldsymbol{M}}^{-1}\tilde{\boldsymbol{N}}, \begin{bmatrix} \tilde{\boldsymbol{X}} & -\tilde{\boldsymbol{Y}} \\ -\tilde{\boldsymbol{N}} & \tilde{\boldsymbol{M}} \end{bmatrix} \begin{bmatrix} \boldsymbol{M} & \boldsymbol{Y} \\ \boldsymbol{N} & \boldsymbol{X} \end{bmatrix} = \boldsymbol{I} \tag{4.1}$$

The procedure described in detail in [4] is followed. The real matrix $\mathbf{F}$ such that $\mathbf{A}_F = \mathbf{A} + \mathbf{BF}$ is stable is chosen using the pole-placement algorithm in MATLAB's *Control System Toolbox*, which makes use of the *Ackerman's Formula* to compute the controller gain matrix $\mathbf{K}$ for which the closed-loop poles of the state-feedback regulator

lie on the desired open-LHP locations. Naturally, in this context, $\mathbf{F}$ is the $\mathbf{K}$. The desired pole locations of $\mathbf{A}_F$ is chosen as $[-2, -2, -1, -1]^T$. A similar thing is done for $\mathbf{H}$, such that $\mathbf{A}_H = \mathbf{A} + \mathbf{HC}$ is stable, but this time using the pole placement function in the context of a state-feedback observer design. The obtained matrices are,

$$\boldsymbol{F} = \begin{bmatrix} -322.0232 & 80.3511 & 42.7952 & 383.8125 \\ -456.2417 & 113.7052 & 62.4080 & 546.3325 \end{bmatrix}$$

$$\boldsymbol{H} = \begin{bmatrix} 40.9207 & -40.0125 \\ 53.8971 & -53.6970 \\ 42.4338 & -42.5641 \\ 16.7635 & -16.4317 \end{bmatrix}$$

Then,

$$\boldsymbol{N}(s) \overset{S}{=} \begin{bmatrix} \boldsymbol{A}_F & \boldsymbol{B} \\ \boldsymbol{C}+\boldsymbol{DF} & \boldsymbol{D} \end{bmatrix}, \tilde{\boldsymbol{N}}(s) \overset{S}{=} \begin{bmatrix} \boldsymbol{A}_H & \boldsymbol{B}+\boldsymbol{HD} \\ \boldsymbol{C} & \boldsymbol{D} \end{bmatrix}$$

$$\boldsymbol{M}(s) \overset{S}{=} \begin{bmatrix} \boldsymbol{A}_F & \boldsymbol{B} \\ \boldsymbol{F} & \boldsymbol{I} \end{bmatrix}, \tilde{\boldsymbol{M}}(s) \overset{S}{=} \begin{bmatrix} \boldsymbol{A}_H & \boldsymbol{H} \\ \boldsymbol{C} & \boldsymbol{I} \end{bmatrix}$$

$$\boldsymbol{X}(s) \overset{S}{=} \begin{bmatrix} \boldsymbol{A}_F & -\boldsymbol{H} \\ \boldsymbol{C}+\boldsymbol{DF} & \boldsymbol{I} \end{bmatrix}, \tilde{\boldsymbol{X}}(s) \overset{S}{=} \begin{bmatrix} \boldsymbol{A}_H & -\boldsymbol{B}-\boldsymbol{HD} \\ \boldsymbol{F} & \boldsymbol{I} \end{bmatrix}$$

$$\boldsymbol{Y}(s) \overset{S}{=} \begin{bmatrix} \boldsymbol{A}_F & -\boldsymbol{H} \\ \boldsymbol{F} & \boldsymbol{O} \end{bmatrix}, \tilde{\boldsymbol{Y}}(s) \overset{S}{=} \begin{bmatrix} \boldsymbol{A}_H & -\boldsymbol{H} \\ \boldsymbol{F} & \boldsymbol{O} \end{bmatrix}$$

All 8 TF matrices obtained belong to $\mathcal{RH}\infty$, and satisfy Equation (4.1).

Question 4.3: Youla parametrization

The set of all real-rational and proper controllers which stabilize an unstable plant $\mathbf{G}(s)$ assuming the feedback configuration described by Figure 1.3 [4] is parametrised as,

$$\boldsymbol{K} = (\boldsymbol{Y} - \boldsymbol{MQ})(\boldsymbol{Y} - \boldsymbol{MQ})^{-1} = (\tilde{\boldsymbol{X}} - \boldsymbol{Q}\tilde{\boldsymbol{N}})^{-1}(\tilde{\boldsymbol{Y}} - \boldsymbol{Q}\tilde{\boldsymbol{M}})$$

where $\mathbf{Q}(s) \in \mathcal{RH}_\infty$. The reduced plant has 2 poles in the open RHP ($s = 0.6951$ and $s = 0.5937$). Let,

$$\boldsymbol{Q}(s) = \begin{bmatrix} \frac{1}{s+1} & 0 \\ 0 & \frac{1}{s+1} \end{bmatrix}$$

The closed-loop transfer functions are always affine functions of $\mathbf{Q}(s)$ like $\mathbf{S} = \mathbf{H}_1 + \mathbf{H}_2\mathbf{Q}\mathbf{H}_3$. A similar procedure, as employed in *Question 2.3* can be used in calculating the sensitivity and complimentary sensitivity transfer functions. Since for the doubly coprime factorizations, positive feedback (1.3) is assumed [4], our closed loop transfer functions will be,

$$\boldsymbol{S}(s) = (\boldsymbol{I} - \boldsymbol{GK})^{-1} = \tilde{\boldsymbol{M}}(\boldsymbol{X} - \tilde{\boldsymbol{N}}\boldsymbol{Q})$$

$$\boldsymbol{T}(s) = \boldsymbol{I} - \boldsymbol{S} = \tilde{\boldsymbol{N}}(\tilde{\boldsymbol{M}}\boldsymbol{Q} - \boldsymbol{Y})$$

As seen in Figure 4.2, both the closed-loop transfer functions show stable responses. We

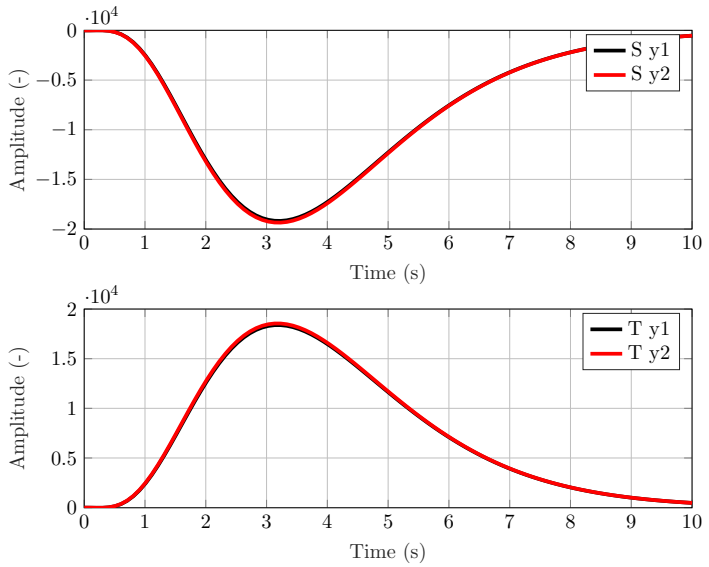

Figure 4.2: Response of **S** and **T** to decaying input, $u = [2e^{-t}\ 0]^T$.

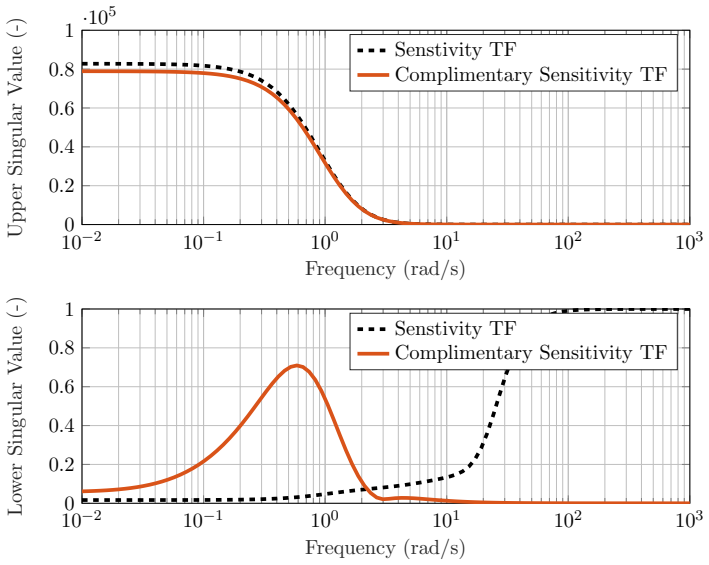

Figure 4.3: Upper and Lower Singular values of **S** and **T**.

can also draw some conclusions regarding the robustness and performance of the controller from Figure 4.3. For frequencies less than 10 rad/s, $\bar{\sigma}(\mathbf{T})$ and $\bar{\sigma}(\mathbf{S})$ are very high, which imply very high sensitivity to input and output channel uncertainties (Chapter 3 in [5]). Additionally, large $\bar{\sigma}(\mathbf{S})$ for low frequencies implies poor controller performance.

Bibliography

[1] F. E. Cellier. Lecture notes on numerical methods for control, April 2001.

[2] B. Dasgupta. *Applied Mathematical Methods*. Pearson, 2012.

[3] J. Doyle, B. Francis, and A. Tannenbaum. *Feedback Control Theory*. Macmillan Publishing Co., 1992.

[4] B. Francis. *A course in H [infinity] control theory*. Springer-Verlag, 1987.

[5] S. Skogestad and I. Postlethwaite. *Multivariable Feedback Control: Analysis and Design*. John Wiley & Sons, 2005.

[6] J. Zhou, Kemin with C. Doyle. *Essentials of Robust Control*. Prentice Hall, 1999.